Solar Phys (2007) 240: 301–313
DOI 10.1007/s11207-006-0259-2

Decametric N Burst: A Consequence of the Interaction of Two Coronal Mass Ejections

P. Démoulin · K.-L. Klein · C.P. Goff · L. van Driel-Gesztelyi · J.L. Culhane · C.H. Mandrini · S.A. Matthews · L.K. Harra

Received: 5 June 2006 / Accepted: 12 November 2006 /
Published online: 27 February 2007

Abstract Radio emissions of electron beams in the solar corona and interplanetary space are tracers of the underlying magnetic configuration and of its evolution. We analyse radio observations from the Culgoora and WIND/WAVES spectrographs, in combination with SOHO/LASCO and SOHO/MDI data, to understand the origin of a type N burst originating from NOAA AR 10540 on January 20, 2004, and its relationship with type II and type III emissions. All bursts are related to the flares and the CME analysed in a previous paper (Goff *et al.*, 2007). A very unusual feature of this event was a decametric type N burst, where a type III-like burst, drifting towards low frequencies (negative drift), changes drift first to positive, then again to negative. At metre wavelengths, *i.e.*, heliocentric distances $\lesssim 1.5 R_\odot$, these bursts are ascribed to electron beams bouncing in a closed loop. Neither U nor N bursts are expected at decametric wavelengths because closed quasi-static loops are not thought to extend to distances $\gg 1.5 R_\odot$. We take the opportunity of the good multi-instrument coverage of this event to analyse the origin of type N bursts in the high corona. Reconnection of the expanding ejecta with the magnetic structure of a previous CME, launched about 8 hours earlier, injects electrons in the same manner as with type III bursts but into open field lines having a local dip and apex. The latter shape was created by magnetic reconnection between the expanding CME and neighbouring (open) streamer field lines. This particular flux tube shape in the high corona, between $5 R_\odot$ and $10 R_\odot$, explains the observed type N burst. Since

P. Démoulin (✉) · K.-L. Klein · L. van Driel-Gesztelyi
Observatoire de Paris, LESIA, UMR 8109 (CNRS), 92195 Meudon Principal Cedex, France
e-mail: pascal.demoulin@obspm.fr

C.P. Goff · L. van Driel-Gesztelyi · J.L. Culhane · S.A. Matthews · L.K. Harra
Mullard Space Science Laboratory, University College London, Holmbury St. Mary, Dorking, Surrey, RH5 6NT, UK

L. van Driel-Gesztelyi
Konkoly Observatory of the Hungarian Academy of Sciences, Budapest, Hungary
e-mail: lvdg@mssl.ucl.ac.uk

C.H. Mandrini
Instituto de Astronomía y Física del Espacio, CONICET-UBA, CC. 67, Suc. 28, 1428 Buenos Aires, Argentina

the required magnetic configuration is only a transient phenomenon formed by reconnection, severe timing and topological constraints are present to form the observed decametric N burst. They are therefore expected to be rare features.

1. Introduction

The structure of the solar corona is defined by closed magnetic fields, providing plasma confinement in active regions, and also flux tubes that are open to interplanetary space. The images taken in X rays and EUV by *Yohkoh*, the *Solar and Heliospheric Observatory* (SOHO), and the *Transition Region And Coronal Explorer* (TRACE) give impressive examples of this structuring in the low corona. It is plausible, and borne out by magnetic field extrapolations, that open magnetic flux tubes become increasingly more important as height increases. Models of the solar wind generally assume that, outside a "source surface" with radius $(2.5-3)R_{\odot}$, the magnetic field is radial in the corotating frame.

The sensitivity of contemporary EUV and X-ray imagers does not allow us to trace magnetic structures at heliocentric distances that exceed, say, $1.5R_{\odot}$. However, spectrography at decimetric and longer radio wavelengths can be used because of the characteristic radio emission of electron beams. When beams of energetic electrons travel through the corona, they may become unstable and amplify Langmuir waves at the local electron plasma frequency. These Langmuir waves can in turn couple into electromagnetic waves at a frequency that, depending on the coupling process, is near the electron plasma frequency or its harmonic. Accordingly, the ensuing radio emission is called fundamental or harmonic emission. Since the waves rapidly decay, the beam produces short-lasting emissions at frequencies that decrease with time, as the beam penetrates to ever greater altitudes, *i.e.*, ever lower ambient densities, in following open magnetic flux tubes. The radio emission generated by this process is called a type III burst. More detailed accounts can be found, *e.g.*, in Suzuki and Dulk (1985). The relationship with electron beams is well established by in situ measurements, as discussed in Lin *et al.* (1986) and Ergun *et al.* (1998).

The radio signature of an electron beam hence traces the evolution of the ambient electron density along the beam path. If such a beam is injected into a coronal loop, the expected signature is that of a type III burst until the beam reaches the summit of the loop. Thereafter, it propagates to higher densities again, and the frequency, instead of continuing to decrease, will increase. The spectral signature in the time – frequency plane is thus a drift to lower frequencies, followed by a drift to higher frequencies. Such a burst is called a "type U" burst, because of its appearance in a dynamic radio spectrum (or it may be termed an inverted U, if the frequency decreases along the ordinate). Imaging observations at decimetric and metric wavelengths confirm this picture (*e.g.*, Aschwanden *et al.*, 1992; Labrum and Stewart, 1970; Sheridan, McLean, and Smerd, 1973; Stewart and Vorpahl, 1977; Aurass, Klein, and Martens, 1994; Aurass and Klein, 1997).

Occasionally, the type U burst signature has been found to be followed by a second type III-like branch, lending to the dynamic spectrum of the emission the form of the letter N. The burst is therefore called a type N burst. This feature was explained by its discoverers (Caroubalos *et al.*, 1987) as the reflection of the electron beam in the converging magnetic field of the coronal loop in the conjugate leg to the acceleration site, an interpretation that was confirmed by the imaging observations of a peculiar event at metre waves (Aurass, Klein, and Martens, 1994).

Type U and N bursts with low-frequency turnover can therefore allow us to identify coronal magnetic loops that peak at large heliocentric distances, or, more generally speaking, curved magnetic flux tubes where the electron beam passes through a local density

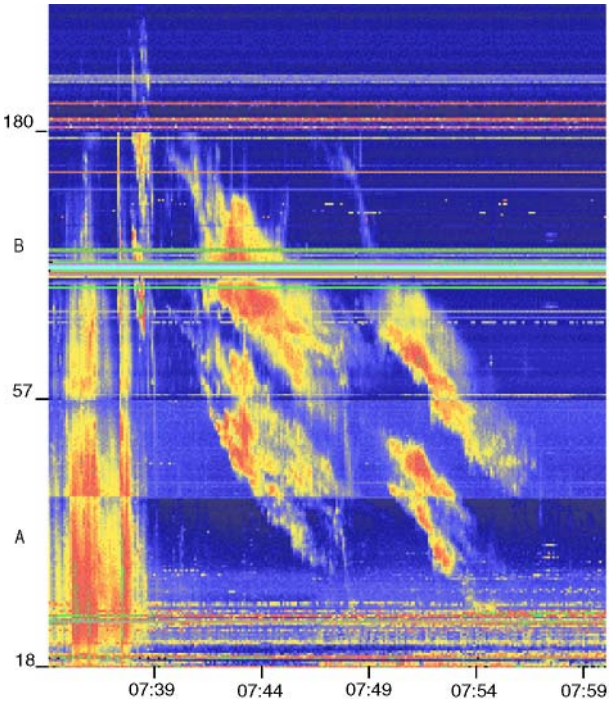

Figure 1 Culgoora dynamic radio spectrum from the January 20, 2004, event (the ordinate scales as the logarithm of the frequency). The intensity increases from dark blue, green, yellow, to red. A group of type III is present on the left of the image (before 07:39 UT). They are followed by two type II bursts, which drift at a similar rate. Both fundamental and first harmonic emissions are present.

minimum. For example, harmonic plasma emission is favored for metric type III and type U bursts. This emission occurs at 180 MHz for an ambient electron density of 10^8 cm^{-3} and at 18 MHz for an ambient density of 10^6 cm^{-3}. In a typical streamer model (Koutchmy, 1994) these densities refer to heliocentric distances of $1.4R_\odot$ and $5R_\odot$, respectively. A systematic inspection of dynamic radio spectra at metre waves by Leblanc, Poquérusse, and Aubier (1983) showed that type U bursts are rarely seen at long metre and decametre wavelengths. Moreover, these authors showed that, in most groups of type U bursts at low frequencies, successive bursts displayed spectral turnovers at ever lower frequencies, which is suggestive of expanding magnetic loops, where the ambient electron density decreases with time. This points to emission in transient loops associated with coronal mass ejections (CMEs).

Since the WAVES spectrograph aboard the Wind spacecraft (Bougeret *et al.*, 1995) has almost closed the gap between spaceborne and ground-based radio observations, only one type U burst observation at frequencies below 10 MHz was published (Leblanc *et al.*, 1999). It occurred during a CME event. These authors gave an account of the few earlier observations, but these had no accompanying coronagraph data. To our knowledge, no type N burst has been detected by spaceborne spectrographs so far.

In the present paper we analyse radio emission, including type III and II bursts at metre wavelengths, and a type N burst observed by the Wind spacecraft during the flares and CME of January 20, 2004. The CME and flares are analysed in detail in the companion paper by Goff *et al.* (2006), hereafter referred to as Paper I.

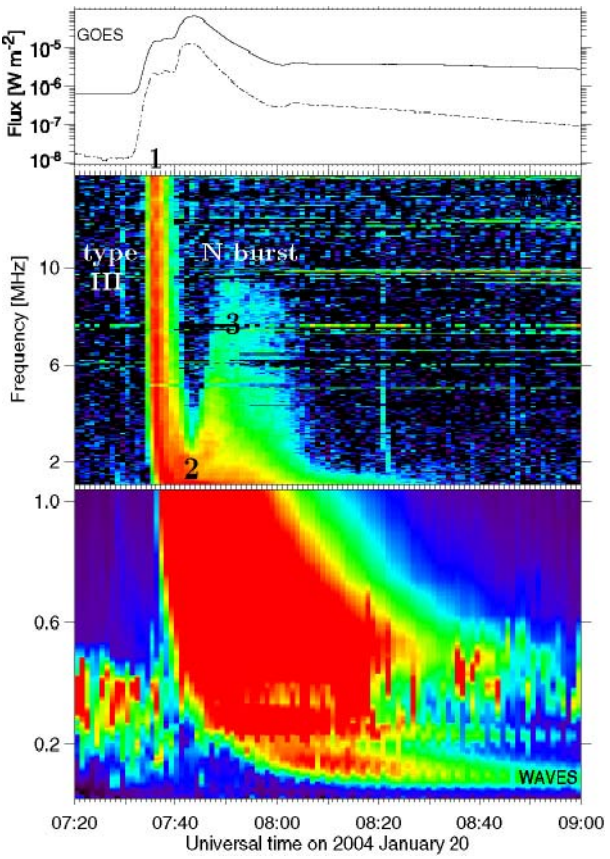

Figure 2 Type III and N bursts observed by the WAVES instrument on the Wind spacecraft (the ordinate scales linearly with the frequency). The GOES light curve is added on the top for reference to the flare evolution. Position 1 indicates an initial type III burst. Position 2 indicates a frequency turnover characteristic of a U burst. Position 3 shows a further turnover. This frequency drift sequence constitutes a type N burst. In the low-frequency range, ≈0.2 – 0.6 MHz, the noisy signal that dominates before 07:40 and after 08:30 UT is auroral emission; on the right, it covers partly the signal of the type N burst.

2. Radio Emission: Electron Beams and Shock Waves in the Middle and High Corona

2.1. Type III Emission

The flares and CME of January 20, 2004, are accompanied by radio emission at metre and longer wavelengths. The Culgoora spectrum shows an initial group of type III bursts starting near 180 MHz (Figure 1, 07:34 – 07:39 UT). Type III emission is seen by the WAVES experiment onboard the Wind spacecraft (Bougeret *et al.*, 1995) at frequencies below 14 MHz (*i.e.*, electron densities below 2.4×10^6 cm^{-3}, Figure 2). The apparently single type III burst in this frequency range results from the merging of the group of bursts at higher frequencies. The type III emission drifts gradually down to frequencies of a few tens of kilohertz, showing that the electron beams propagate well into interplanetary space. This radio emission shows electrons escaping from the corona along open magnetic field lines.

2.2. Type II Emission

The metric type III bursts in Figure 1 are followed by type II emission (07:39 – 07:56 UT) with several drifting bands. The fact that type II emission drifts more slowly towards lower frequencies than type III emission reveals an exciter slower than electron beams. Type II

bursts are considered as the radio signature of shock waves propagating through the corona (see reviews by Nelson and Melrose, 1985; Mann, 1995; Aurass, 1997).

Two clearly separated bands are seen in the type II burst between 07:40 UT and 07:48 UT, followed by a gap in emission, and then by two other bands between 07:50 UT and 07:56 UT (Figure 1). The frequency axis of the dynamic spectrum is logarithmic, and the frequency drift of the type II lanes can be approximated by a straight line. The relative drift rate inferred from a linear fit can be related to an exponential density model, as follows. If the electron density decreases exponentially with height (Koutchmy, 1994), and assuming that the shock wave generating the type II burst moves opposite to the gravitational density gradient, we can infer the relative drift rate from this fit to be related to the exciter speed υ and the scale height H through $\frac{1}{\nu}\frac{\mathrm{d}\nu}{\mathrm{d}t} = -\frac{\upsilon}{2H}$. Note that this determination of the exciter speed is independent of the hypothesis of fundamental and harmonic plasma emission and also does not require us to assume an electron density at the base of the corona. However, we must specify the scale height. For a hydrostatic coronal scale height (10^5 km in the low corona, scaling as the square of heliocentric distance) at a heliocentric distance of $(1.5-2)R_\odot$, the relative drift rate measured on the spectrogram between about 200 and 18 MHz ($\mathrm{d}\log_{10}\nu/\mathrm{d}t = -8.10\times10^{-4}\ \mathrm{s}^{-1}$) implies an exciter speed in the range 840–1500 km s^{-1}.

2.3. Type N Burst in the High Corona

In the WAVES frequency band the initial type III burst is followed by emission whose dynamic spectrum is reminiscent of a metric type N burst (Caroubalos *et al.*, 1987). The emission has the initial characteristics of type III (positions 1 to 2 in Figure 2), but after 07:42 UT the high-frequency end of the spectrum first drifts towards higher frequencies (positions 2 to 3), then after 07:48 UT, it again towards lower frequencies (after position 3). Hereafter we will refer to the branch between 1 and 2 as the first ascending branch, between 2 and 3 as the descending branch, and after 3 as the second ascending branch of the type N burst, respectively.

Interpreting the WAVES spectrum is difficult because the low-frequency spectrum does not show distinctive traces of the type N burst. It is well known that apparently structureless type III bursts at these low frequencies often correspond to a series of type III bursts at higher frequencies (Poquérusse *et al.*, 1996). The emissions of different electron beams apparently merge into a quasi-continuous spectral feature. However, the reversal of the frequency drift at position 2 is readily visible. The spectrum therefore shows a type U burst whose rising branch is partly coincident with the end of the initial type III burst. It cannot be definitely excluded that the renewed negative drift after position 3 is produced by independent new type III bursts. The daily spectrogram of WAVES (http://cdpp.cesr.fr/) shows indeed numerous type III bursts, and some of them start in the 2 – 14 MHz range. But their trailing edge drifts much faster than that of the emission after position 3. Moreover, the superposition of two type III bursts, shifted in time, only has drifts towards higher frequencies. Therefore we are left with a simple alternative: Either the observed feature is a type N burst, whose spectral characteristics are to be interpreted in terms of a single exciter, or we are observing a series of type III bursts whose starting frequencies after position 3 are tuned by chance in such a way as to mimic a single feature with slowly drifting high-frequency cutoff. In the following we take the view that the negative frequency drift after position 3 reveals the same electron beams as the preceding type U burst, so we are observing indeed a type N burst.

A rough estimate of the exciter speed can be obtained from the frequency drift rate, *i.e.* 6 minutes to go from 3 MHz (position 2) to 7 MHz (position 3). By using the relative drift rate at the centre frequency between the turnovers, *i.e.* 5 MHz, and an exponential density

model as above, the speed of the exciter of the radio burst is $\upsilon = \frac{2H}{\nu}\frac{\Delta\nu}{\Delta t} = 440(\frac{r}{R_\odot})^2$ km s^{-1}. The electron density at the summit of the flux tube, which from the turnover frequency is 10^5 cm^{-3} for fundamental emission and 3×10^4 cm^{-3} for harmonic emission, is typical for equatorial regions at heliocentric distances of about $5R_\odot$ and for streamers at heliocentric distances exceeding $10R_\odot$ (Koutchmy, 1994). This range implies an exciter speed in the descending branch of the type N burst of between 11 000 and 44 000 km s^{-1} ($0.04-0.15c$), which is about the range of exciter speeds of type III bursts in the solar corona and interplanetary space (*e.g.*, Buttighoffer, 1998). This confirms our interpretation of the spectral feature as the signature of an electron beam that propagates along a sunward curved magnetic flux tube.

The second ascending branch drifts rather slowly to lower frequencies (with a drift rate reduced by about a factor 10 with respect to the first ascending branch). It extends to about 0.5 MHz, which means that the emission fades at much higher frequencies than the previous type III burst (Section 2.1). This implies that the type N emission is much more strongly absorbed in the interplanetary medium than the type III burst emission, most likely because the electron beams of the type N burst travel away from the spacecraft and the radio emission has a much longer path than the previous type III burst. This is the case if the type III burst is emitted by electron beams that travel along the Earth-connected Parker spiral, while the type N emitting beams propagate along a Parker spiral that is rooted farther eastwards, and therefore bends away from Earth.

Interpreting the spectrum with its succession of negative and positive frequency drifts as a signature of a disturbance propagating along a coronal flux tube, we obtain the following constraints:

(i) From the first turnover frequency of the spectrum (position 2 in Figure 2), the electron beams encounter a local minimum in the ambient electron density near 07:42 UT, where the plasma frequency or its harmonic is about 3 MHz ($\geq 5R_\odot$). This may be the summit of a magnetic flux tube.
(ii) From the second turnover frequency (position 3), the local plasma frequency or its harmonic is 7 MHz ($\geq 3R_\odot$). The electrons reach this point at 07:48 UT.

3. Physical Interpretation of Radio Data

In Paper I, we analysed a series of flares (two flares of GOES class M and one class C) and a CME observed on January 20, 2004, occurring in close succession in NOAA 10540. The three flares (or three phases of the complex event) were separated both temporally and spatially but also with an overlap and physical connection between consecutive events. Each phase had four main flare kernels with configurations similar to previously analysed confined flares. Magnetic reconnection proceeded stepwise, along the AR inversion line, producing the first two flares. These two phases are associated with the CME lift-off observed by the *Large Angle and Spectroscopic Coronagraph* (LASCO, Brueckner *et al.*, 1995). The third flare (phase III, an LDE) was interpreted as a relaxation of the magnetic configuration, which, in phases I and II, had been subjected to forced reconnection by the expanding magnetic structure of the CME. In the following sections, we interpret all the radio observations described in Section 2 with reference to the magnetic evolution of flares/CME analysed in Paper I and another CME, which erupted eight hours earlier.

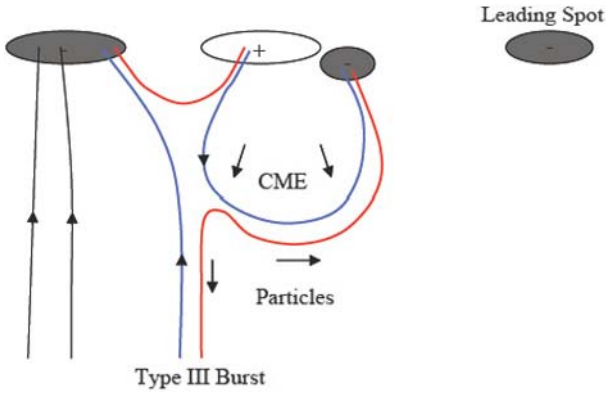

Figure 3 Schematic view of the main magnetic polarities and field line connections involved in the large-scale reconnection. The expanding magnetic structure (CME) reaches the oppositely directed magnetic structure of the streamer east of the flaring AR (blue lines). The resulting reconnection process leads to loop formation interconnecting the two neighbouring magnetic polarities and the formation of large-scale "open" field lines (red lines), along which particles accelerated during the reconnection process propagate. The upward traveling electrons from this site produce type III bursts, whereas the downward traveling electrons emit reverse-slope bursts.

3.1. Type III Bursts

The group of type III bursts occurred in phase I of the flare, indicating that, in the early part of the flare, electrons are accelerated along open field lines. This is indeed a frequent characteristic of flares. Pick *et al.* (2005) interpreted this behavior in eruptive flares as a consequence of the reconnection in current sheets built during the pre-flare evolution between closed (AR) and open (streamer) field lines. Such a reconnection scenario for the expanding magnetic structure with the surrounding open field is summarized in Figure 3 for the event studied here. (The magnetic configuration is deduced from MDI and EIT data and from magnetic extrapolation as explained in Paper I.)

3.2. Type II Bursts

The low-frequency cutoff at decametre waves (about 20 MHz) shows that either the type II bursts are from flare-related shocks, be they blast waves or initially piston driven, or the eruptive magnetic configuration mostly accelerates electrons at low altitudes in the corona.

The two sets of type II lanes could be two distinct bursts, each composed of emission at the local plasma frequency and its harmonic. This view is corroborated by the timing, since the difference between the onset times of the two type II bursts equals the time interval between the starts of phases I and II of the complex flare (see Paper I). However, we cannot exclude the possibility that the high-frequency band of the first period and the low-frequency band of the second period might belong to the same drifting feature, because they can be easily related by a straight line in the dynamic spectrogram. In this case the high-frequency band of the second period would correspond to the emission at the second harmonic of the local plasma frequency.

The presence of two successive type II bursts with similar characteristics is rarely observed (see Subramanian and Ebenezer, 2006). In both these interpretations, their similar

drifting velocity suggests that they were excited by the same expanding structure. The conditions for radio emission had probably been met in different parts of the shock at different times, for example, owing to a nonmonotonic spatial distribution of the Alfvén velocity (Vršnak *et al.*, 2002).

The velocities deduced for the type II bursts are high (840 – 1500 km s^{-1}) when compared with the CME velocities projected in the plane of sky that are obtained later from C2 and C3 observations (300 – 560 km s^{-1}). However, the CME was launched close to the disk centre (at a distance $\approx 0.3 R_{\odot}$). This implies a radial CME speed a factor ≈ 3 larger, which is indeed compatible with the velocity deduced from the type II bursts.

3.3. Type N Burst: Difficulties with Magnetic Mirroring

The classical interpretation of the first turnover point in the frequency drift, corresponding to a type U burst, requires the presence of a closed loop. However, closed magnetic structures are not expected to exist at heliocentric distances above a few solar radii. A further problem is the type N burst. Type N bursts at metric wavelengths are usually interpreted as being due to the mirroring of electron beams (Caroubalos *et al.*, 1987). In the present event mirroring could occur at the coronal shock revealed by the metric type II burst or in the legs of a large-scale magnetic loop. We will now show that both interpretations are contradicted by the data and that a more likely interpretation involves the transient magnetic field configuration that develops in the course of a former CME.

The simultaneous occurrence of a type II burst might suggest that the electron beam is reflected at the shock when the latter intersects the remote leg of a transient loop in which a type U electron beam propagates. However, this interpretation is inconsistent with the fact that the type II burst appears at much higher frequencies at that time than the turnover frequency of the type N burst (position 3 in Figure 2).

Magnetic mirroring of an electron beam is not a likely candidate for the second turnover at ≈ 7 MHz in the burst under discussion, since it would require a strong magnetic field high above the photosphere. From the previous height estimates, and assuming conservation of the magnetic moment of the electrons, we find that the magnetic field at the presumed mirror point at a heliocentric distance $\geq 3 R_{\odot}$ should be comparable to the magnetic field in the region where the type III radiation starts, *i.e.*, around $1.5 R_{\odot}$ ($\nu = 180$ MHz, Figure 1). The magnetic field is expected to decrease like a magnetic dipole at these large distances, so let us assume that the field decreases with the third power of heliocentric distance in each leg of the hypothetical large-scale loop. This would imply that the field strength in the conjugate leg of the large-scale loop, at a similar height as the starting point of the type III bursts, would be at least 8 times stronger than in the region where the type III bursts start. Such a magnetic field imbalance is not plausible in the low-beta plasma of the corona.

A second argument that casts doubt on magnetic mirroring comes from the drift rates of the type N burst. We have already noted that the second ascending branch of the type N burst, after position 3, drifts more slowly than the preceding descending branch, whereas one would expect similar absolute values of the drift rates from magnetic mirroring, where the electrons would traverse the same plasma successively in two opposite directions.

An easy explanation of the different drift rates is that the electrons travel successively through magnetic structures with different inclinations with respect to the radial direction. The presence of field lines extending from the Sun to a maximum height, then returning, before going out again (now with a magnetic dip) could account for both the change in propagation direction and the variable drift speed. In this interpretation the electrons are not mirrored, but they simply follow the particular shape of field lines. However, we need to

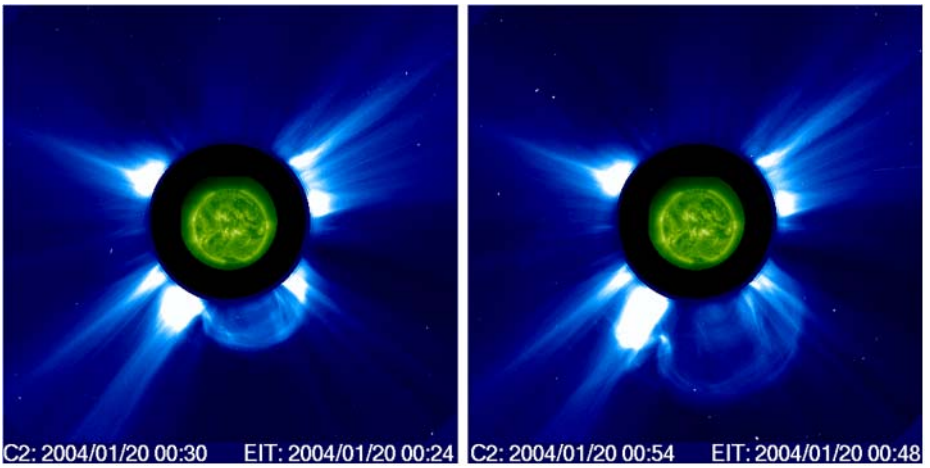

Figure 4 The "midnight" CME, which originated from AR 10540 about eight hours prior to the radio emissions studied in this paper. The "midnight" CME interacted with the eastward streamer. (In particular, there is an inverse U-shaped structure in emission in between the streamer and the CME.)

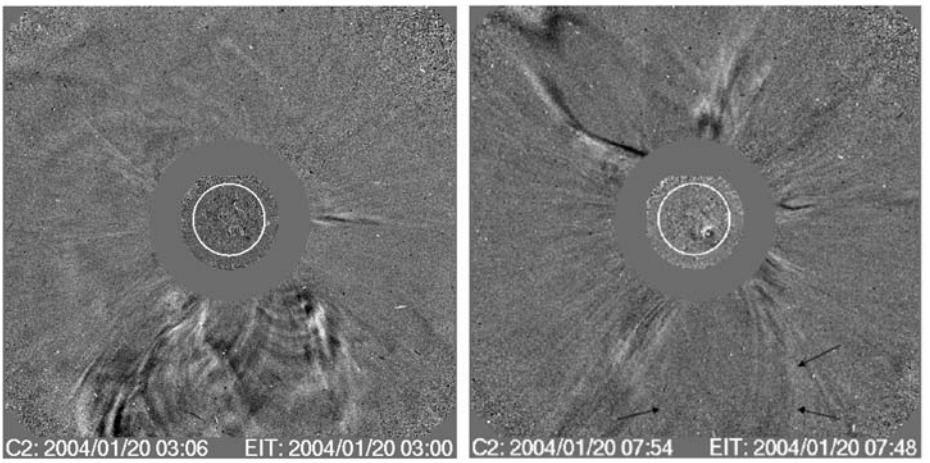

Figure 5 The "midnight" halo CME lasted for several hours in the C2 field of view. A large number of loops kept expanding from the Sun, showing continuous signs of interaction with the eastward streamer (see Appendix). The last expanding loop detectable is extending to about $6R_{\odot}$ in the right panel (black arrows). It is present at the time when the radio N burst is observed.

understand how such a large dipped arch-like magnetic structure could have formed having an apex at heliocentric distance $\geq 5R_{\odot}$.

3.4. A Previous CME and Its Role

A significant halo CME occurred at 00:06 UT on January 20, 2004, in association with a long-duration GOES C-class flare that began at 23:08 UT on January 19. We call this event the "midnight" CME. It has been studied by Fazakerley *et al.* (2005), who also analysed its arrival at Earth over two days later. Selected LASCO C2 images taken in the interval

following the detection of the halo CME are shown in Figure 4. This CME comes from the northern part of the AR 10540, which produced later, in its southern part, the CME studied in Paper I (at ≈8 UT) and the radio emission studied in this paper.

The outward expansion of the magnetic structure does not stop after the leading edge and the void structure of the CME leave the C2 field of view. Indeed, difference images indicate the formation of a complex array of closed loop-like structures that expand away from the limb, for several hours following the onset of the CME. For example, the expanded structures that existed at around 03:06 and 07:54 UT are shown in Figure 5. A large closed structure with apex at $\approx 6 R_{\odot}$ is present at 07:54 UT. It appears to be the last of the series of expanding loops belonging to the "midnight" CME.

Fazakerley *et al.* (2005) demonstrated that the expanding front of the 00:06 UT halo CME interacted with the eastward streamer. The interaction, shown in Figure 4, shows that the streamer extension decreased as the CME expanded and pushed against it. There is also evidence of an inverse U-shaped structure in white-light emission at the CME – streamer interface. This unusual structure in a CME is most likely outlining the reconnected field lines between the expanding CME and the streamer open field configuration (Figure 6, top).

Another CME occurred later (at ≈8 UT) in the southern part of AR 10540, associated with the radio emissions studied in this paper. In Paper I, we show that this CME has a similar interaction with the streamer. For this second CME, the reconnection scenario is further supported by the EUV observations of shrinking interconnecting loops in between the following polarity of the AR and the westward unipolar region (the western footpoint region of the streamer, as sketched in Figure 3). Since both CMEs came from the same globally bipolar AR, they have the same global magnetic configuration. Hence, both CMEs are expected to reconnect with the open field of the streamer.

From all of this observational evidence we conclude that the "midnight" CME interaction with the streamer produced unusual magnetic field lines with dips at large heights in the corona, as sketched in the top panel of Figure 6.

3.5. Type N Burst: Electrons Tracing a Transient and Dipped Magnetic Flux Tube Within a CME?

We conclude in Section 3.3 that any scenario ascribing the type N emission to magnetic mirroring in a closed loop is inconsistent with the observed radio emission drifts. Thus, the most plausible interpretation relies on the shape of the field lines having a very specific configuration involving the two CMEs. The partial reconnection of the magnetic structure of the "midnight" CME with open field lines could indeed establish special magnetic paths for some of the electron beams, which can lead to a type N burst as explained in the following.

The second CME started in the special magnetic environment created by the still ongoing "midnight" CME. At the western side of the AR, part of the erupting magnetic structure expands, pushing against the still anchored leg of the "midnight" CME. While starting from the same AR, some evidence is presented in Paper I (*cf.* Figures 8 and 10) that these two CMEs come from different parts of the AR having opposite magnetic helicity. This increases the difference in the field orientation between the two CME magnetic configurations. A finite angle between the magnetic field of these structures permits the formation of current sheets, in which reconnection starts somewhat later, injecting accelerated electrons in the large-scale field lines just like in the type III burst process (Figure 6). However, in this case the special shape of the previously reconnected field lines in the "midnight" CME forces the electrons to return towards higher density regions in the Sun (after the local apex

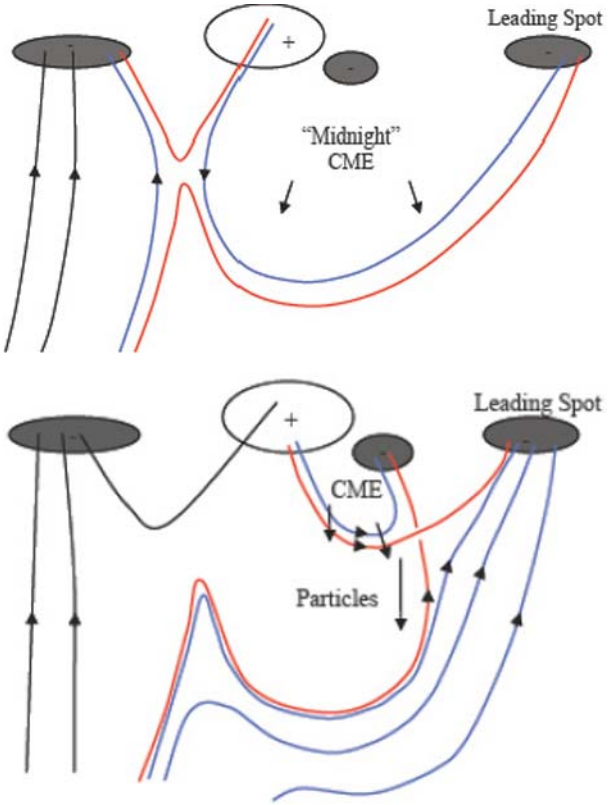

Figure 6 Cartoons showing the mechanism leading to the N burst. Top panel: Formation of the dipped large-scale field lines during the "midnight" halo CME event. Note that successive loop expansions resulting from this CME continued for several hours (Figure 5). Bottom panel: Reconnection between magnetic loops of the two CMEs (at "midnight" and ≈8 UT) injected accelerated electrons into the huge dipped field lines, leading to an N burst (Figure 2). Pre-reconnected field lines are in blue, and reconnected field lines are in red; some extra field lines are added in black to outline the surrounding magnetic configuration.

is reached), then later to flow away again (after the dip is reached). So we suggest that, unlike metre-wave type N bursts, the decametre-wave type N burst under discussion does not show mirroring of electrons but is due to the peculiar transient geometry of field lines that participate in the magnetic restructuring during the former CME.

The type N burst occurs in close time coincidence with the initial type III emission, which suggests that the electron beams producing the two burst types are accelerated in neighbouring regions. Moreover, the field lines, having reconnected early enough with the streamer in the "midnight" event, are able to straighten out as follows. By taking an Alfven speed of the order of 500 km s^{-1} (Mann et al., 2003; Warmuth and Mann, 2005), a magnetic disturbance propagates a solar radius in about twenty minutes, so that the dip in reconnected field lines is only expected to be present during a time interval of the order of one hour. Then, the second CME could interact with both dipped field lines and straightened field lines from the previous CME, as well as with remaining open field lines from the streamer. The injection of electrons in the dipped field lines, located more to the east, gives the type N burst, whereas the injection in the straightened out field lines gives the type III bursts (Figures 3 and 6). A range of field lines with a varying degree of curvature is present between these two extremes, and we suggest that injections of electrons in these field lines give the continuum of emission seen in between the type III bursts and the higher frequency border of the type N burst in Figure 2 (around 7:38 UT at 2 MHz).

4. Conclusion

Fast-drift radio bursts with frequency turnovers (type U bursts) are rarely found at decametre and longer wavelengths, and type N features have not been reported at these wavelengths before. The reason most generally invoked is the absence of closed magnetic structures at large heliocentric distances. Previous studies (Leblanc, Poquérusse, and Aubier, 1983; Leblanc *et al.*, 1999, and references therein) ascribed low-frequency type U bursts to electron beams in loops that expand in the course of a CME.

The January 20, 2004, CME provides a new example for this general idea, with two new observational ingredients: (i) From the analysis of the flare, the two CMEs, and the global magnetic field configuration in Paper I, we have gained insight into the structure and evolution of the magnetic topology; (ii) the peculiarity of the decametre radio spectrum shows with certainty a type U burst, and probably a type N burst, and allows us at the same time to exclude the interpretation of magnetic mirroring of electron beams on physical grounds. Moreover, we find evidence for reconnection of the erupting magnetic configuration with the neighbouring streamer: interconnecting loops (observed with the *Extreme-ultraviolet Imaging Telescope*, EIT) and open field lines with dips (a U-shaped brightening, concave outwards, seen in LASCO/C2 in the interaction region between the "midnight" CME and its eastward streamer). Therefore, we have several indications that the unusual type N burst can be ascribed to a peculiar transient magnetic field configuration.

We conclude that the type N burst has basically the same physical origin as type III bursts — *i.e.*, the result of freely propagating electron beams — but it needs a very specially shaped open magnetic field configuration to occur. The expansion of magnetic loops and their interaction with the streamer is initiated, about 8 hours before, by a previous CME originating from the same AR. Its magnetic field configuration reconnected partially with a neighbouring open field region. This interaction lasted for several hours. Then, the second CME configuration reconnects both with the streamer and the previous CME configuration, accelerating electrons onto a set of field lines ranging from nearly radial to dipped. This creates type III and N emission at decametre waves with a continuum of emitting structures in between these two limiting cases (Figure 2). Given the need for all these temporal, spatial, and topological constraints, it is not surprising that observations of type U and type N bursts at decametre wavelengths are rare. The probability of detecting such bursts should be greater in ARs with a high level of CME productivity, such as occurs during a strong emergence phase and/or in a nest of activity.

Acknowledgements The authors are grateful to H. Aurass and M. Kaiser for helpful discussions and to the referee for constructive comments. The authors thank the SOHO/MDI, LASCO, EIT, and TRACE consortia and the Culgoora Radio Observatory for their data. The CME movies are from the CME catalog generated and maintained at the CDAW Data Center by NASA and the Catholic University of America in cooperation with the Naval Research Laboratory. SOHO is a joint project by ESA and NASA. C.H.M. is grateful for a PPARC funded visitor's grant. C.H.M. acknowledges support from the following Argentinean grants: UBACyT X329 (UBA), PICT 12187 (ANPCyT), and PIP 6220 (CONICET). C.H.M. and P.D. acknowledge financial support from CNRS (France) and CONICET (Argentina) through their cooperative science program (05ARG0011, No. 18302). L.V.D.G. acknowledges the Hungarian government grant OTKA 048961. J.L.C. thanks the Leverhulme Trust for the award of a Leverhulme Emeritus Fellowship.

Appendix

Movies of the CMEs observed by LASCO C2 and C3 (c2_rdif.html, c3_rdif.html) are available from http://cdaw.gsfc.nasa.gov/CME_list/daily_movies/2004/01/20/. The disturbance of the streamer by the "midnight" CME is best seen in the movie c2eit.html at this URL.

References

Aschwanden, M.J., Bastian, T.S., Benz, A.O., Brosius, J.W.: 1992, *Astrophys. J.* **391**, 380.

Aurass, H. 1997, In: Trottet, G. (ed.) *Coronal Physics from Radio and Space Observations*, *Lecture Notes in Physics*, vol. **483**, Springer-Verlag, Berlin, p. 135.

Aurass, H., Klein, K.-L.: 1997, *Astron. Astrophys. Suppl.* **123**, 279.

Aurass, H., Klein, K.-L., Martens, P.C.H.: 1994, *Sol. Phys.* **155**, 203.

Bougeret, J.-L., *et al.*: 1995, *Space Sci. Rev.* **71**, 231.

Brueckner, G.E., *et al.*: 1995, *Solar Phys.* **162**, 357.

Buttighoffer, A.: 1998, *Astron. Astrophys.* **335**, 295.

Caroubalos, C., Poquérusse, M., Bougeret, J.-L., Crepel, R.: 1987, *Astrophys. J.* **319**, 503.

Ergun, R.E., *et al.*: 1998, *Astrophys. J.* **503**, 435.

Fazakerley, A.N., *et al.*: 2005, *Geophys. Res. Lett.* **32**, L13105.

Goff, C.P., van Driel-Gesztelyi, L., Démoulin, P., Culhane, J.L., Matthews, S.A., Harra, L.K., Mandrini, C.H., Klein, K.L., Kurokawa, H.: 2006, *Solar Phys.*, DOI 10.1007/s11207-007-0260-4.

Koutchmy, S.: 1994, *Adv. Space Res.* **14**(4), 29.

Labrum, N.R., Stewart, R.T.: 1970, *Proc. Astron. Soc. Aust.* **1**, 316.

Leblanc, Y., Dulk, G.A., Kaiser, M.L., Bougeret, J.-L.: 1999, *Geophys. Res. Lett.* **26**, 1089.

Leblanc, Y., Poquérusse, M., Aubier, M.G.: 1983, *Astron. Astrophys.* **123**, 307.

Lin, R.P., Levedahl, W.K., Lotko, W., Gurnett, D.A., Scarf, F.L.: 1986, *Astrophys. J.* **308**, 954.

Mann, G.: 1995. In: Benz, A., Krüger, A. (eds.) *Coronal Magnetic Energy Releases*, *Lecture Notes in Physics*, vol. **444**, Springer-Verlag, Berlin, p. 183.

Mann, G., Klassen, A., Aurass, H., Classen, H.-T.: 2003, *Astron. Astrophys.* **400**, 329.

Nelson, G.J., Melrose, D.B.: 1985. In: McLean, D., Labrum, N. (eds.) *Solar Radiophysics: Studies of Emission from the Sun at Meter Wavelengths*, Cambridge University Press, Cambridge, p. 333.

Pick, M., Démoulin, P., Krucker, S., Malandraki, O., Maia, D.: 2005, *Astrophys. J.* **625**, 1019.

Poquérusse, M., Hoang, S., Bougeret, J.-L., Moncuquet, M.: 1996, In: Winterhalter, D., Gosling, J.T., Habbal, S.R., Kurth, W.S., Neugebauer, M. (eds.) *Solar Wind Eight*, AIP Press, Woodbury, p. 62.

Sheridan, K.V., McLean, D.J., Smerd, S.F.: 1973, *Astrophys. J.* **15**, L139.

Stewart, R.T., Vorpahl, J.: 1977, *Solar Phys.* **55**, 111.

Subramanian, K.R., Ebenezer, E.: 2006, *Astron. Astrophys.* **451**, 683.

Suzuki, S., Dulk, G.A.: 1985, In: McLean, D., Labrum, N. (eds.) *Solar Radiophysics: Studies of Emission from the Sun at Meter Wavelengths*, Cambridge University Press, Cambridge, p. 289.

Vršnak, B., Magdalenić, J., Aurass, H., Mann, G.: 2002, *Astron. Astrophys.* **396**, 673.

Warmuth, A., Mann, G.: 2005, *Astron. Astrophys.* **435**, 1123.